PERGAMON

Vision Research 39 (1999) 4361–4377

Vision Research

www.elsevier.com/locate/visres

A multiscale spatial filtering account of the White effect, simultaneous brightness contrast and grating induction☆

Barbara Blakeslee *, Mark E. McCourt

Department of Psychology, North Dakota State University, Fargo, ND 58105-5075, USA

Received 28 October 1998; received in revised form 4 March 1999

Abstract

Blakeslee and McCourt ((1997) *Vision Research*, *37*, 2849–2869) demonstrated that a multiscale array of two-dimensional difference-of-Gaussian (DOG) filters provided a simple but powerful model for explaining a number of seemingly complex features of grating induction (GI), while simultaneously encompassing salient features of brightness induction in simultaneous brightness contrast (SBC), brightness assimilation and Hermann Grid stimuli. The DOG model (and isotropic contrast models in general) cannot, however, account for another important group of brightness effects which includes the White effect (White (1979) *Perception*, *8*, 413–416) and the demonstrations of Todorovic ((1997) *Perception*, *26*, 379–395). This paper introduces an oriented DOG (ODOG) model which differs from the DOG model in that the filters are anisotropic and their outputs are pooled nonlinearly. The ODOG model qualitatively predicts the appearance of the test patches in the White effect, the Todorovic demonstration, GI and SBC, while quantitatively predicting the relative magnitudes of these brightness effects as measured psychophysically using brightness matching. The model also accounts for both the smooth transition in test patch brightness seen in the White effect (White & White (1985) *Vision Research*, *25*, 1331–1335) when the relative phase of the test patch is varied relative to the inducing grating, and for the spatial variation of brightness across the test patch as measured using point-by-point brightness matching. Finally, the model predicts intensive aspects of brightness induction measured in a series of Todorovic stimuli as the arms of the test crosses are lengthened (Pessoa, Baratoff, Neumann & Todorokov (1998) *Investigative Ophthalmology and Visual Science*, *Supplement*, *39*, S159), but fails in one condition. Although it is concluded that higher-level perceptual grouping factors may play a role in determining brightness in this instance, in general the psychophysical results and ODOG modeling argue strongly that the induced brightness phenomena of SBC, GI, the White effect and the Todorovic demonstration, primarily reflect early-stage cortical filtering operations in the visual system.

Keywords: Brightness induction; White effect; Simultaneous brightness contrast; Grating induction

1. Introduction

It has long been known that the brightness of a region of visual space is not related solely to that region's luminance, but depends also upon the luminances of adjacent regions (for review see Kingdom, 1997). A well-known demonstration of this is simultaneous brightness contrast (SBC). SBC is usually described as a homogeneous brightness change within an enclosed test patch such that a gray patch on a white background looks darker than an equiluminant gray patch on a black background. This effect has been well quantified with respect to inducing background and test patch luminance (Heinemann, 1955). Although SBC decreases with increasing test patch size, brightness induction occurs for test patches as large as 10° (Yund & Armington, 1975). Since this distance far exceeds the dimensions of retinal or LGN receptive fields in monkey (DeValois & Pease, 1971; Yund, Snodderly, Hepler & DeValois, 1977; DeValois & DeValois, 1988), a common explanation for SBC has been that the brightness of the test patch is determined by the information at the edges of the bounded region (for example, by average perimeter contrast) and is subsequently filled-in or assigned to the entire enclosed area (Cornsweet & Teller, 1965; Shapley & Enroth-Cugell, 1984; Grossberg & Todorovic, 1988; Paradiso & Nakayama, 1991; Par-

☆ Supported by NSF (IBN-9514201).

* Corresponding author. Fax: +1-701-231-8426.

E-mail address: blakesle@prairie.nodak.edu (B. Blakeslee)

0042-6989/99/$ - see front matter

PII: S0042-6989(99)00119-4

adiso & Hahn, 1996; Rossi & Paradiso, 1996; for review see Kingdom & Moulden, 1988). Grating induction (GI), in contrast to SBC, is a brightness effect that produces a spatial brightness variation (a grating) in an extended test patch (McCourt, 1982). The perceived contrast of the induced grating decreases with increasing inducing grating frequency and with increasing test patch height (McCourt, 1982; Foley & McCourt, 1985). GI, like SBC, extends over large distances since it is still observed in test patches at least as large as 6° (Blakeslee & McCourt, 1997). Unlike SBC, however, homogeneous brightness fill-in cannot account for GI since it cannot produce a pattern in the extended test patch. Blakeslee and McCourt (1997) measured brightness induction as a function of changing test patch height and width such that their stimuli included both SBC and GI configurations. They demonstrated that both the structure and magnitude of brightness induction were parsimoniously accounted for by the output of a differentially weighted, octave-interval array of seven difference-of-Gaussian (DOG) filters. This array of filters differed from those previously employed to model GI (Moulden & Kingdom, 1991) and the early filtering stages of the visual system (Wilson & Bergen, 1979; Watt & Morgan, 1985; Kingdom & Moulden, 1992) in that it included filters tuned to significantly lower spatial frequencies. The decision to include such low frequency filters is supported by recent physiological evidence that spatial integration occurs over comparably large distances in primary visual cortex of both cat (Rossi, Rittenhouse & Paradiso, 1996) and monkey (Gilbert, Das, Ito, Kapadia & Westheimer, 1996). It is significant that this relatively simple filtering explanation, which was the first to simultaneously account for both GI and SBC, could be generalized to account for several other important brightness phenomena, such as the GI demonstrations of Zaidi (1989), the Shapley and Reid (1985) contrast and assimilation demonstration, and the induced spots seen at the street intersections of the Hermann Grid. Thus, the DOG model (Blakeslee & McCourt, 1997) provided a powerful tool that integrated a number of seemingly diverse brightness phenomena with a history of different explanations.

The present paper specifically addresses a group of effects, including the White effect (White, 1979) and a demonstration of Todorovic (1997), which cannot be accounted for by isotropic contrast models such as the DOG model and the edge-dependent models discussed earlier. In the White effect gray test patches of identical luminance placed on the black and white bars of a squarewave grating appear different in brightness. What makes the effect so interesting, however, is that the direction of the effect is independent of the aspect ratio of the test patch. This means that, unlike SBC and GI, the White effect does not depend on the amount of black or white border in immediate contact with the test patch or in its general vicinity. For example, when the gray patch is a vertically oriented rectangle sitting on the white stripe of a vertical grating, it has two short sides that are in contact with the coaxial white bar it is sitting on and two long sides that are in contact with the flanking black bars (see Fig. 2). Despite the more extensive black borders the gray patch appears *darker* than an equivalent gray patch sitting on a black stripe. In other words, rather than contrasting with a weighted sum of its borders or the surrounding area, the gray patch appears to contrast with the bar upon which it is situated, largely independent of the flanking stripes. A similar effect is seen in the Todorovic (1997) demonstration shown in Fig. 9b. Despite the fact that the black and white squares that overlap the test patch have the same amount of contact with the test patches as the backgrounds, the test patch on the black background with the overlapping white squares appears brighter than the test patch on the white background with the overlapping black squares.

A number of qualitative explanations have been offered for the White effect. White proposed a mechanism called 'pattern-specific inhibition' (White, 1981) based on the notion that elongated cortical filters having similar preferred orientation and spatial frequency selectivity, and which received their input from adjacent retinal locations, might tend to inhibit each other and thus produce the effect. In a similar vein Foley and McCourt (1985) suggested that hypercomplex-like cortical filters with small centers and elongated surrounds might be responsible for the effect. Moulden and Kingdom (1989) proposed a dual mechanism model based on their psychophysical investigation of the effect of varying the height of both the flanking and coaxial inducing bars. They concluded that a local mechanism, mediated by circularly symmetric center-surround receptive fields, operated along the borders of the test patch and produced a particularly strong signal at the corner intersections of the test patch with the coaxial bar. According to their model it is this corner signal that in some (unspecified) manner disproportionately weights the coaxial bar relative to the flank and induces brightness into the test patch. Additionally, a more spatially extensive mechanism was required to allow the coaxial bar to exert an influence on the brightness of the test patch throughout its length. This mechanism was seen as possibly implicating the operation of neurons with small centers and elongated surrounds similar to those proposed by Foley and McCourt (1985).

Numerous attempts have also been made to explain the White effect on the basis of higher level perceptual inferences involving depth and the Gestalt notion of 'belongingness' (Agostini & Proffitt, 1993; Spehar, Gilchrist & Arend, 1995; Taya, Ehrenstein & Cavonius, 1995; Pessoa & Ross, 1996; Gilchrist, Kossifydis, Bonato, Agostini, Cataliotti, Li & et al., 1999). Recent

work by Zaidi, Spehar and Shy (1997), however, indicates that the White effect is observed irrespective of any three-dimensional interpretation and independently of any perceptual inferences of coplanarity or 'belongingness'. Some question remains whether this is true when display luminances exceed the range of reflectances of common objects (i.e. 30:1) under homogeneous illumination (Gilchrist, Bonato, Annan & Economou, 1998).

Both Zaidi et al. (1997) and Todorovic (1997) argue convincingly that an explanation based on an analysis of local junctions in the stimulus, specifically T-junctions in the case of the White effect, can account for a number of brightness effects. A T-junction is defined as the meeting place of three regions. Two of the regions (those that form the stem of the T-junction) are termed collinear regions. The third region, called the flanking region, forms the top of the T-junction. Todorovic (1997) and Zaidi et al. (1997) demonstrate that the brightness of regions that share edges with several other regions and whose corners involve T-junctions is predominantly dependent on the luminance of collinear regions and is in the direction of a SBC effect. In the White effect the flanking bars form the tops of the four T-junctions that define the corners of the test patch. The stems of the T-junctions are formed by the test patch and the coaxial bar on which it is superimposed. The T-junction rule appears to have some generality in that it also qualitatively accounts for the brightness of test patches in other novel brightness displays (Todorovic, 1997; Zaidi et al., 1997) that cannot be explained by isotropic contrast models.

Although the T-junction analysis is impressive and offers a useful predictive rule for the set of stimuli to which it applies, it falls short of identifying an underlying mechanism. This paper presents a mechanistic explanation for a variety of brightness effects in the form of an oriented DOG (ODOG) multiscale spatial filtering model. The ODOG model differs from the DOG model of Blakeslee and McCourt (1997) in that the filters are anisotropic and their outputs are pooled nonlinearly. The ODOG model qualitatively predicts the relative brightness of the test patches in the White effect, a Todorovic demonstration, GI and SBC and quantitatively predicts the relative magnitudes of these brightness effects as measured psychophysically using brightness matching. Note that a T-junction analysis makes no predictions for the test patches of either GI or SBC stimuli. In further tests the ODOG model was able to account for the smooth transition in mean brightness seen in the White effect when the relative phase of the test patch was varied relative to the inducing grating (White & White, 1985). Significantly, this smooth transition is not readily explained by a T-junction analysis. In addition, point-by-point brightness matching revealed brightness variations across the test patches of these White stimuli that are in accord with model predictions. Finally, the model also accounts for the brightness induction measured in a series of Todorovic stimuli as the arms of the test crosses are lengthened (Pessoa, Baratoff, Neumann & Todorovic, 1998). The model fails in one condition that is successfully predicted by a T-junction analysis. It is concluded that higher-level perceptual grouping factors may in this instance play a role in determining brightness, but that generally the induced brightness effects of SBC, GI the White effect and the Todorovic demonstration primarily reflect the operations of early-stage cortical filtering.

2. General methods

2.1. Subjects

Two subjects (the authors BB and MM) participated in the present experiments. Both subjects were well-practiced psychophysical observers and possessed normal or corrected-to-normal vision.

2.2. Stimuli

Stimuli were generated on a PC compatible microcomputer (Pentium 150) with a custom modified Cambridge VSG board (Vision Research Graphics Inc.). Images were presented on a high-resolution display monitor (21'' IDEK Iiyama Vision Master, model MF-8221). Display format was 1024 (w) $\times$ 768 (h) pixels. Frame refresh rate was 97 Hz (non-interlaced). All images could possess 2^8 simultaneously presentable linearized intensity levels selected from a palette of approximately 2^{12}. Subjects viewed the display from a distance of 60.7 cm resulting in a stimulus field that was 24.2° in height and 32° in width. Individual pixels measured 0.031° $\times$ 0.031°. Inducing patterns appeared in the lower half of the stimulus field while the upper half of the stimulus display contained a matching stimulus of adjustable luminance surrounded by a homogeneous field set to the mean luminance of the display (50 cd/m^2).

2.3. Procedures

All stimuli were viewed binocularly through natural pupils in a dimly lit room. Subjects' heads were positioned relative to the display with a chin and forehead rest. Eye movements were restricted only in that subjects were instructed to maintain their gaze within the illuminated display to hold adaptation state stable. A standard matching technique was used to measure the magnitude of induction in the various brightness displays. A comparison of brightness matching and can-

cellation (nulling) techniques was performed previously by McCourt and Blakeslee (1994). They found that brightness measures obtained using these two methods were equally informative and were lawfully related. In general, a brightness null corresponds to the point on the complete brightness matching function where variations in induced brightness are cancelled by the addition or subtraction of luminance(s) within the test patch. The brightness matches referred to in the present study correspond to another point on the complete brightness matching function; they are a direct measure of the brightness of the test patch when it is set to the mean luminance of the display. The matching stimulus was a patch measuring either $1° \times 1°$ or $3° \times 3°$ such that it corresponded in size to the test patch of the stimulus configuration under examination. A button press from the subject initiated each matching trial. The initial value of the matching stimulus was randomized at the beginning of each adjustment trial and subjects controlled subsequent increments and/or decrements in matching luminance by selecting and depressing appropriate response buttons. Each button press resulted in a maximal luminance change of 1%. The adjustment interval for each trial lasted until the subject indicated that the match was complete by pressing the 'done' button. Final adjustment settings were recorded by the computer, which also randomized the presentation of stimuli. Between 5 and 15 matching settings were obtained in each experimental condition from each subject. In experiment 3 a point-by-point matching technique was used (Heinemann, 1972; McCourt, 1994; Blakeslee & McCourt, 1997). This technique differed from the standard matching technique in that the matching patch was narrow, 0.25° in width by 3.0° in height, and occupied one of 14, rather than one of two, spatial positions. Subjects adjusted the luminance of the matching patch until it appeared to match that portion of the test patch located directly below. Thus, brightness matches could be obtained for different horizontal locations across the test patch.

In this paper we were concerned only with brightness, the perceived luminance or intensity of a stimulus. Subjects were specifically instructed to match brightness (the perceived intensity of light) and not lightness (the perceived reflectance of a surface) or brightness contrast (relative brightness).

3. The oriented DOG (ODOG) model

The ODOG model is an extension of the DOG filtering model of Blakeslee and McCourt (1997) which consisted of an array of seven isotropic two-dimensional DOG filters whose center frequencies were arranged at octave intervals (from 0.1 to 6.5 c/d). The ratio of center/surround space constants was 1:2, producing filters whose spatial frequency bandwidth (full-width at half-height) was 1.9 octaves. Center/surround volumes were equal, such that the response of each DOG to a homogeneous field was zero. The sensitivities of the filters in the array were summed after being differentially weighted according to a power function of spatial frequency with a slope of 0.1. This weighting is consistent with the shallow low-frequency falloff of the suprathreshold CSF that was expected to be associated with the suprathreshold contrast stimuli that were used to develop the model (Georgeson & Sullivan, 1975).

The ODOG filters differ from the DOG filters in that they are anisotropic. The oriented filters were produced by setting the ratio of DOG center/surround space constants to 1:2 in one orientation and to 1:1 in the orthogonal orientation (see Table 1). A gray level representation of such an ODOG filter appears in Fig. 1a. Note that although the center remains circular, the surround extends beyond the center for a distance of twice the center size in one orientation but is the same size as the center in the orthogonal orientation. These filters can be described as either end-stopped Gaussian blobs or as simple-like cells (such as those found in the cortex of monkey or cat) that are orientation and spatial frequency selective. The ODOG model is implemented in six orientations (0°, 30°, 60°, 90° $-30°$ and $-60°$). Each orientation is represented by seven volume-balanced filters that possess center frequencies arranged at octave intervals (from 0.1 to 6.5 c/d). Their spatial frequency tuning and bandwidth of 1.9 octaves (in the orientation orthogonal to their spatial elongation) is the same as that of the DOG filters in the Blakeslee and McCourt (1997) model. It should be noted that the particular filter center frequencies which were selected are not critical: any octave-interval (or denser) array of filters, with comparable bandwidth, which spans a comparable range of frequency will produce essentially identical pooled responses. The seven spatial frequency filters (Fig. 1b) within each orientation are summed after weighting across frequency using a power function with a slope of 0.1 (Fig.

Table 1
Oriented difference of Gaussian space constants

Mechanism	Space constant (°)			
	Center		Surround	
	X	Y	X	Y
1	0.047	0.047	0.047	0.093
2	0.094	0.094	0.094	0.188
3	0.188	0.188	0.188	0.375
4	0.375	0.375	0.375	0.75
5	0.75	0.75	0.75	1.5
6	1.5	1.5	1.5	3
7	3	3	3	6

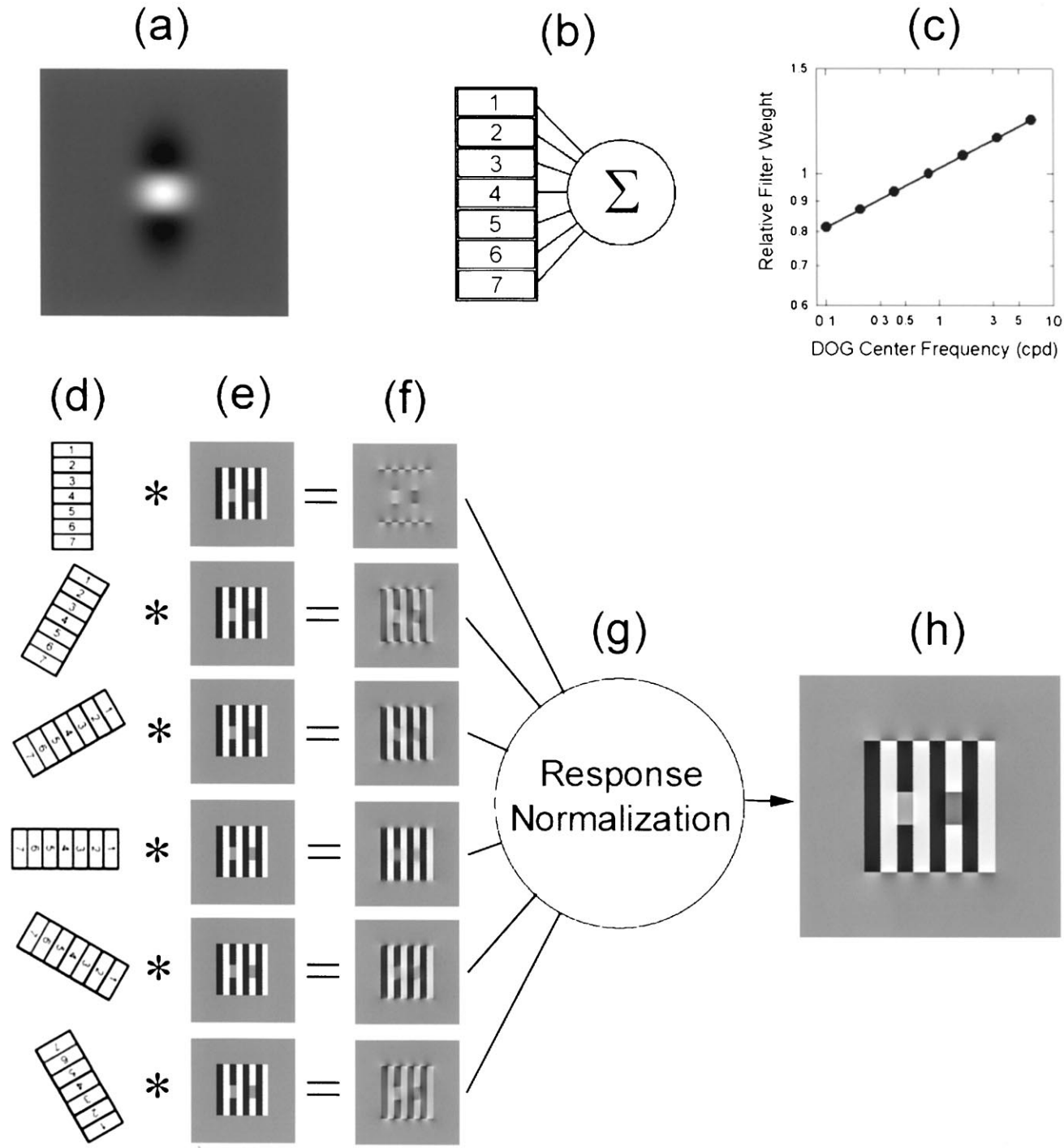

Fig. 1. A diagrammatic representation of the ODOG model. (a) A gray level representation of an oriented difference-of-Gaussian (ODOG) filter. (b) Seven filters, with center frequencies spaced at octave intervals, are summed within orientation after being weighted across frequency (c) using a power function with a slope of 0.1. (d) The resulting six multiscale spatial filters, one for each orientation, are convolved with stimuli of interest (e). (f) The convolution outputs are normalized and pooled across orientation according to their space-averaged root-mean-square (RMS) activity level (f–g) to produce a resultant output (h).

1c). This is the slope that was used to weight the filters in the original DOG model (Blakeslee & McCourt, 1997) and is again consistent with the shallow low-frequency fall-off of the suprathreshold CSF that is expected to be associated with the high-contrast stimuli that are under investigation. The resulting six multiscale spatial filters, one per orientation, are convolved with the stimulus of interest (Fig. 1d–e). The filter outputs (Fig. 1f) are pooled across orientation according to their space-averaged root-mean-square (RMS) activity

level, as computed across the entire image. The pooling is in accord with a simple response normalization in which the filter outputs are weighted such that the RMS activity levels across orientation channels are equated (Fig. 1g). This form of pooling was adopted after preliminary modeling results indicated that it produced the desired outcome of simultaneously accounting for the White effect and GI. Response nonlinearities found in neurons in cat and monkey visual cortex, such as contrast gain control and the rapidly accelerating increase in response at low contrast, may represent the physiological substrate for this type of response normalization (for overview see Geisler & Albrecht, 1995). Finally, an important feature of the ODOG model is that it reduces to the linear isotropic DOG model (Blakeslee & McCourt, 1997) when the stimuli are themselves spatially isotropic. In this case the ODOG RMS response levels are equivalent (or nearly so) at all orientations and are therefore unaffected by subsequent normalization. The ODOG filters were chosen specifically to preserve this link to the previous model.

4. Modeling demonstration 1: the ODOG model predictions for White's effect, GI, SBC and a Todorovic demonstration

Fig. 2 depicts the White effect for two different combinations of inducing grating spatial frequency and test patch size. The ODOG model predictions for these stimuli appear in the right-hand panels. In each panel, the dashed gray line is the veridical luminance profile of the stimulus across the horizontal center of the test patch, and the solid line represents a slice of the model output along this same line. For the stimulus luminance profile the values ranging between 0 and 255 on the vertical axis represent 256 linear luminance steps from 0 to 100 cd/m^2. For the model output the 256 steps represent a range of 1150 model units. It is important to note that this scaling is constant for all of the modeling demonstrations in this paper allowing them to be compared in a relative manner. In both stimuli the test patch situated on the white bar appears darker than the test patch situated on the black bar despite the test patch on the white bar having more extensive contact with the black flanking bars, and vice versa. The ODOG model output clearly predicts the brightness of

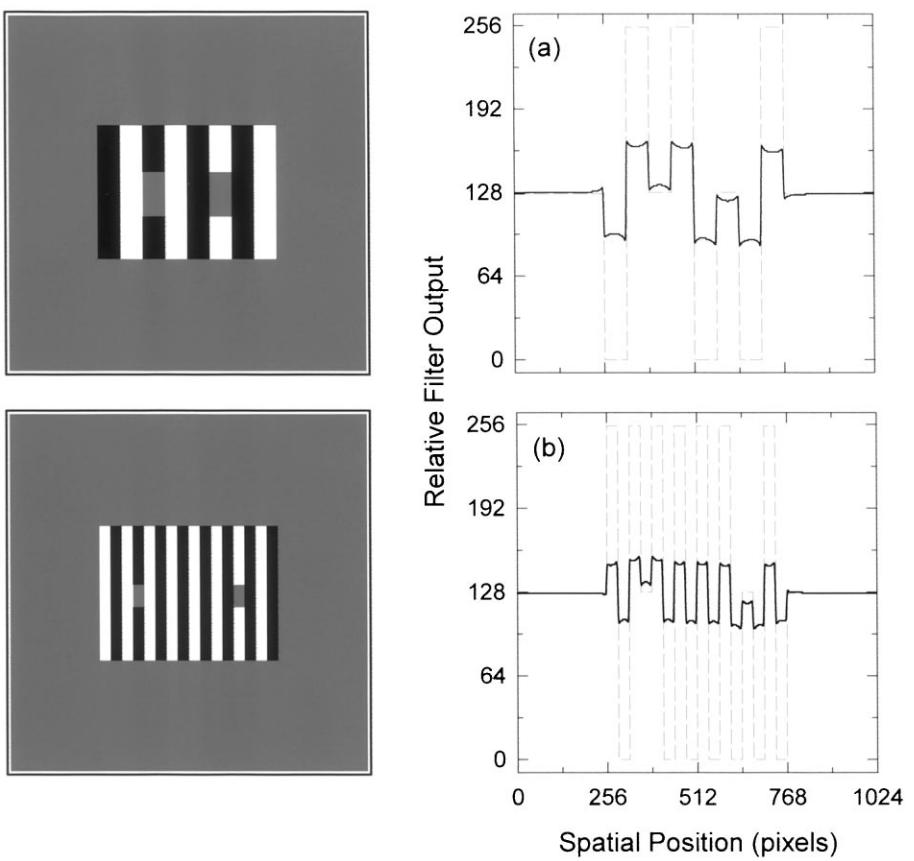

Fig. 2. White stimuli illustrating two combinations of inducing grating spatial frequency and test patch size. The output of the ODOG model in response to these stimuli appears in the right-hand panels. In each panel the dashed gray line refers to the veridical luminance profile of the stimulus across the horizontal center of the test patch and the solid line represents a slice of the model output along this same line. In both stimuli the test patch situated on the white bar appears darker than the test patch situated on the black bar despite the test patch on the white bar having more extensive contact with the black flanking bars. The ODOG model outputs are clearly in accord with the appearance of the test patches.

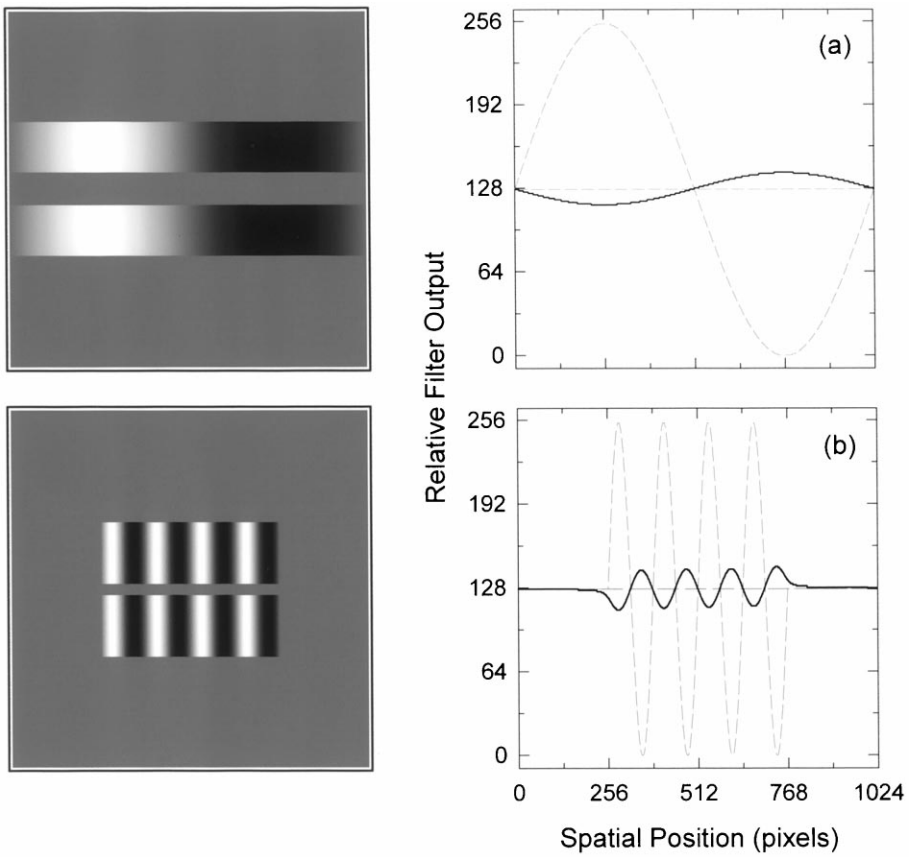

Fig. 3. Grating induction (GI) for two different combinations of inducing grating spatial frequency and width, and test patch height and width. The ODOG model output was obtained using the same parameter values as in Fig. 2, The horizontal dashed gray line is the veridical luminance profile of the stimulus test patch. The other dashed gray line is the luminance profile of the inducing grating. The output of the ODOG model (solid line) correctly predicts the appearance of a counterphase grating in the homogeneous test patch (GI).

the test patches. Some insight into the model is gained by noting that when the multiscale ODOG filter is in the orientation depicted in Fig. 1(a), there is very little response to the inducing grating. When the filter is centered on the test patch situated on the white bar, inhibition from the white bar results in a smaller response from the filter than when it is situated on a similar test patch on a black bar. In other words, the filter output predicts the White effect (see top panel in Fig. 1f) because the test patches contrast with the bars on which they are situated, largely independent of the flanking stripes. The filter in the orthogonal orientation (see fourth panel from top in Fig. 1f), produces a large response to the inducing grating, and a response to the test patches that is opposite to the White effect, i.e. the test patches contrast with the lateral stripes. Normalization of the RMS filter outputs across orientation produces a pooled response portrait which predicts the White effect because the filters that produce the White effect produce larger responses to the test patches *relative to their overall activity* than do the filters that produce the lateral contrast effect.

Fig. 3 illustrates grating induction (GI) for two different combinations of inducing grating spatial frequency and width, and test patch height and width. The ODOG model predictions were obtained using the same parameter values as in Fig. 2. The horizontal dashed gray line is the veridical luminance profile of the stimulus test patch. The second dashed gray line is the luminance profile of the inducing grating. The output of the ODOG model (solid line) correctly predicts the appearance of a counterphase grating in the homogeneous test patch (GI). Fig. 4 shows SBC for two test patch sizes and the ODOG model predictions, again using the same parameter values as in Fig. 2. The output of the model correctly predicts the SBC effect; the test patch on the black background appears brighter than the test patch on the white background. Finally, Fig. 9b demonstrates that the model can also predict the relative brightness of the test patches in a Todorovic (1997) demonstration. Notice that the test patch on the black background appears brighter than the test patch on the white background despite the fact that the test patch on the black background has the same amount of border contact with the black background and with the white overlapping squares.

These demonstrations clearly show that the ODOG model can predict the relative brightness of the test patches in two effects, the White effect and a Todorovic demonstration, that have resisted explanation based on isotropic contrast models. Importantly, it can also encompass SBC and GI, effects that have been successfully modeled with the isotropic DOG model (Blakeslee & McCourt, 1997). Thus, these four diverse brightness effects can be understood in terms of a common mechanism.

It is important to note that the predicted brightness profile for the test patches is not truly homogeneous in any of these demonstrations. Blakeslee and McCourt (1997) quantified these inhomogeneities in the brightness profiles of the test patches of GI and SBC stimuli using a point-by-point brightness matching technique. The profiles were well predicted by the non-oriented DOG model. The ODOG model predictions for SBC and GI are similar and also account for the earlier point-by-point brightness matching data. Point-by-point brightness matches for the White effect are the topic of experiment 2.

5. Experiment 1: the relative magnitudes of SBC, GI, White's effect and the Todorovic demonstration

The previous demonstrations indicate that the ODOG model can qualitatively predict the relative brightness of the test patches within four different brightness effects. The following psychophysical brightness matching experiment was conducted to obtain quantitative data on the relative magnitudes of induction across this set of brightness effects. The results provide data regarding the relative magnitudes of these effects under similar conditions and provide a test of whether the ODOG model can quantitatively predict their relative magnitudes. Although, as discussed previously, brightness induction in the test patches was not completely homogeneous, subjects found it relatively easy to set a single value for the matching patch representing the overall appearance of the test patch. SBC stimuli were produced using one cycle of a 0.03 cyc/deg square wave grating as the inducing background. Both 1° and 3° square test patch conditions

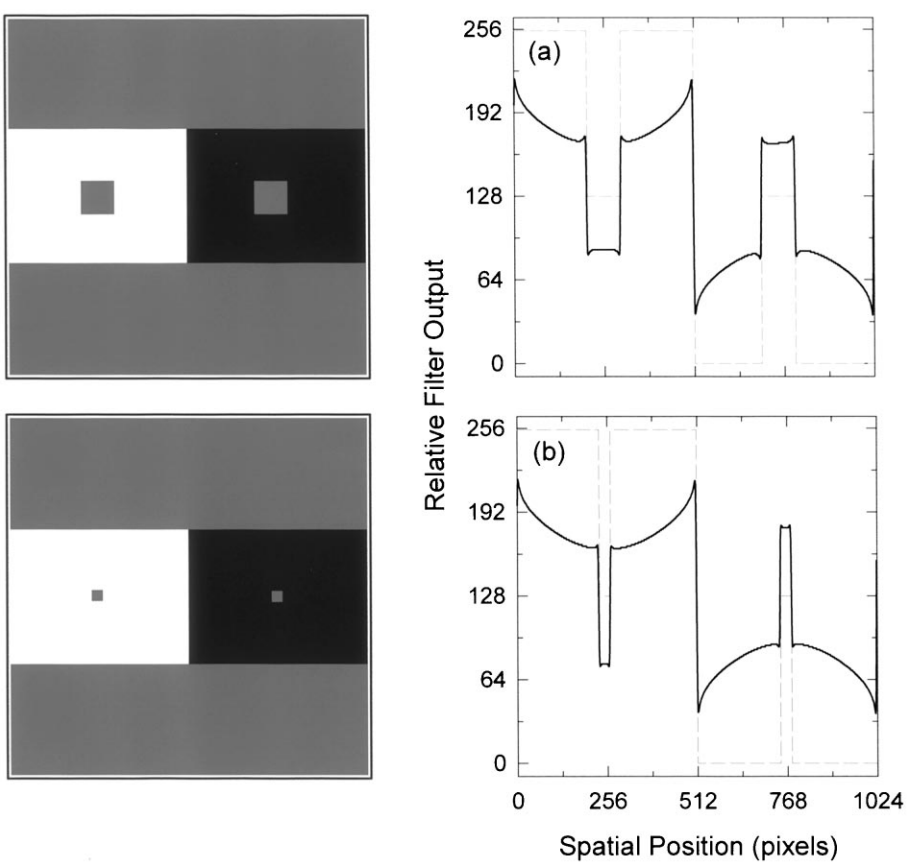

Fig. 4. Simultaneous brightness contrast (SBC) stimuli for two test patch sizes along with ODOG model output, using the same model parameter values as in Fig. 2. The output of the model correctly predicts the direction and relative magnitude of the SBC effect; the test patch on the black background appears brighter than the test patch on the white background, and the effect is greater for the smaller test patches.

were studied (Fig. 4). The Todorovic (1997) stimulus tested was identical to the SBC stimulus with the 3° test patches, but included the addition of four white squares overlapping the corners of the gray test patches on the black background and four corresponding black squares on the white background. The size of the four overlapping squares was 3° × 3° and matched the size of the test patches (Fig. 9b). GI stimuli consisted of either a 0.03 cyc/deg sine wave inducing grating with a 3° test field height and a 32° test field and inducing field width (Fig. 3a) or a 0.125 cyc/deg sine wave inducing grating with a 1° test field height and a 16° test field and inducing field width (Fig. 3b). White stimuli were composed of square-wave inducing patterns of either 0.25 cyc/deg (Fig. 2a) or 0.5 cyc/deg (Fig. 2b). Test patch width corresponded to one-half the cycle width, i.e. it matched the bar width, of the inducing grating. For the 0.25 cyc/deg inducing grating, test patch width was 2° and test patch height was 4°. For the 0.5 cyc/deg inducing grating, test patch width was 1° and test patch height was 2°. Inducing patterns of 100% contrast were used in all brightness displays.

5.1. Results and discussion

The bar graph in Fig. 5 (left ordinate) depicts the mean deviation of the matching luminance from the mean luminance (as a proportion of the mean luminance) for the various brightness conditions. Data from the two subjects are plotted separately in the two panels.

The horizontal lines dividing each bar at the 0.0 point represent the luminance of the test patches, which were set to the mean luminance of the display (50 cd/m^2). The bars extending above and below the mean luminance indicate each subject's mean brightness matches to the two different test patches in each stimulus condition, and the error bars represent the 95% confidence limits for each mean match. The first brightness matches depicted are those to SBC stimuli with test patches measuring 3° (SBC3) and 1° (SBC1), respectively. The bars extending above the mean represent brightness matches for test patches on the dark background (which appear brighter than the mean) and the bars extending below the mean represent the test patch matches on the bright background (which appear darker than the mean). The data indicate that the magnitude of brightness induction (defined to include both brightness and darkness induction) in SBC displays is greater for the smaller test patches. This result is in accord with the previous literature (Yund & Armington, 1975).

Next are the matches for the two GI displays: the 0.03 cyc/deg sine wave inducing grating with a test field height of 3° (GI3) and the 0.125 cyc/deg sine wave inducing grating with a test field height of 1° (GI1). The brightness matches in this instance are to an area around the peak and trough of the induced grating that is of the same extent as the matching patch (3° and 1°, respectively). As expected from previous research which showed that GI magnitude decreases with increasing inducing spatial frequency and test field height (Foley & McCourt, 1985), the predicted decrease in induction resulting from a higher spatial frequency inducing grat-

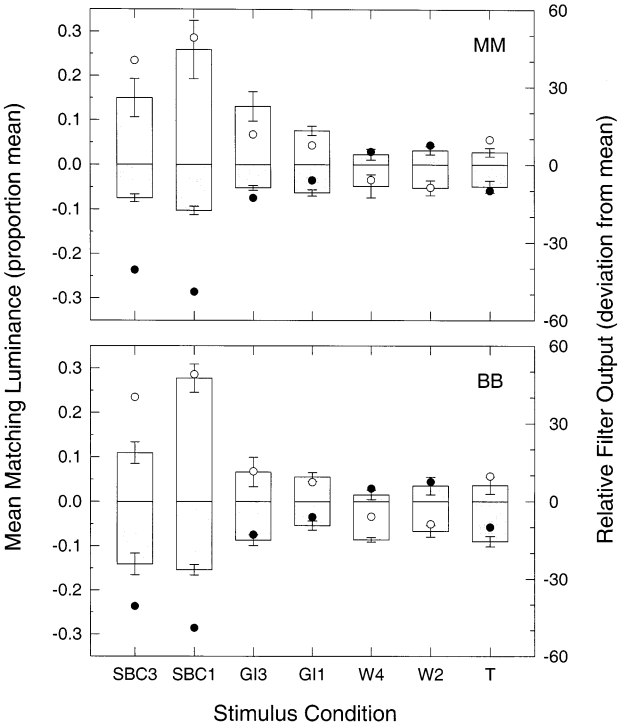

Fig. 5. The bar graph (read against left ordinate) illustrates the mean deviation of matching luminance from the mean luminance (expressed as a proportion of mean luminance) for the various stimulus conditions. The error bars are 95% confidence limits. Data from the two subjects are plotted separately in the upper and lower panels. The first brightness matches depicted are matches to the test patches of SBC stimuli with 3° (SBC3) and 1° (SBC1) test patches, respectively. The bars extending above the mean represent brightness matches for test patches on the dark background (which appear brighter than the mean), while the bars extending below the mean represent the test patch matches on the bright background (which appear darker than the mean). Next are matches for the two GI displays: the 0.03 cyc/deg sine wave inducing grating with a test field height of 3° (GI3), and the 0.125 cyc/deg sine wave inducing grating with a test field height of 1° (GI1). The conditions (W4), 4° test field height, and (W2), 2° test field height, depict the magnitude of the White effect on the 0.25 and 0.5 cyc/deg square wave inducing gratings, respectively. Note that for these two conditions the bars extending above the line represent matches to test patches located on the dark bars of the inducing grating while those below the line are matches to the test patches located on the bright bars of the inducing grating. The final condition (T) plots the magnitude of brightness induction in the Todorovic stimulus. The bar extending above the mean luminance represents the match to the test patch on the dark inducing background with the overlapping white squares. The bar extending below the mean is the match to the test patch on the white background with the overlapping black squares. The symbols refer to the right-hand ordinate and represent the ODOG model predictions for each stimulus. The filled symbols are the predictions for the matches that appear as dark bars and the open symbols are the predictions for the matches that appear as white bars.

ing is offset by the expected increase in induction due to the smaller test field height. Overall, however, the data argue for slightly greater brightness induction in the (GI3) condition.

The conditions labeled (W4), 4° test field height and (W2), 2° test field height, depict the magnitude of the White effect on the 0.25 and 0.5 cyc/deg square wave inducing gratings, respectively. Note that for these two conditions the bars extending above the mean represent matches to test patches located on the dark bars of the inducing grating while those extending below the mean are matches to the test patches located on the bright bars of the inducing grating. The size of the effect appears quite similar for the two White stimuli. The size of the White effect is also similar to that measured by Zaidi, Spehar and Shy (1997) using brightness matching.

The last condition, labeled (T), describes brightness induction in the Todorovic stimulus (Todorovic, 1997). The bar extending above the mean luminance represents the match to the test patch on the dark inducing background with the overlapping white squares. The bar extending below the mean is the match to the test patch on the white background with the overlapping black squares.

The circular symbols in Fig. 5 refer to the right-hand ordinate and represent the ODOG model predictions for each stimulus. The filled symbols are the predictions for the matches that appear as dark bars and the open symbols are the predictions for the matches that appear as white bars. To arrive at this single-valued prediction the model output was averaged across the width of the test patches. In the case of GI, model output was averaged across a distance corresponding to the width of the matching patch in that condition (1° or 3°), centered on the position in the test field corresponding to the peak or trough of the inducing grating. Note that although this metric is convenient for the present purposes, neither the predicted nor the observed brightness profiles are single-valued over these distances. It is nevertheless impressive that in addition to predicting the qualitative appearance of the test fields in the various stimuli, the ODOG model also does a credible job of predicting the *relative magnitudes* of brightness induction across this diverse array of stimulus displays (Fig. 5).

Although it is not further discussed in this paper, it is worth noting that the magnitudes of brightness and darkness induction are asymmetrical for many of the stimulus displays and in some instances differ between observers (Fig. 5). While these asymmetries are not captured by the ODOG model as it is presently implemented, permitting different gain parameters to be applied to the outputs of independent on- and off-channels would constitute a logical first step towards accommodating these differences.

6. Modeling demonstration 2: effects of test patch phase on White's effect

As discussed earlier, Todorovic (1997) and Zaidi et al. (1997) emphasized the importance of T-junctions in predicting the brightness of test patches in a number of brightness illusions including the White effect. Todorovic (1997) acknowledged, however, that an earlier study by White and White (1985) revealed a major problem for the local T-junction analysis. White and White (1985) manipulated the phase of the gray test regions relative to the inducing bars of the White (1979) display. A designation of 0° phase was arbitrarily assigned when the gray test bars were collinear with the black bars of the inducing grating and 180° phase when they were collinear with the white bars. In addition, four other equally spaced phase relations of 36°, 72°, 108° and 144° phase were tested. The results showed a nearly linear relationship between the brightness and the phase of the gray test patches. The test patches were judged darker for greater phase-differences between the test patches and the black bars of the flanking grating. Thus, discontinuous changes in T-junction structure did not result in discontinuous changes in brightness. The following modeling demonstration was used to determine if the ODOG model could give a better account of this smooth transition in brightness that cannot easily be explained on the basis of T-junctions.

Fig. 6 illustrates various phases of the test patches relative to the inducing bars of a 0.25 cyc/deg square-wave inducing grating with test patches measuring 2° in width and 4° in height. Note that the stimulus in Fig. 6a (the 0° phase relationship for the gray test patch on the black bar and the 180° phase relationship for the test patch on the white bar) is identical to that in Fig. 2a. In Fig. 6b the test patches have been shifted to the right by 16 pixels (0.5°). Relative to the black bar, this corresponds to a phase shift of 45° for the test patch on the left, and 135° for the test patch on the right. Figure 6c shows the test patches shifted by 32 pixels, or 1.0°, corresponding to a phase shift of 90° for the test patch on the left relative to the black bar. The right hand panels illustrate the ODOG model output to the three displays. Fig. 7 plots the output of the ODOG model averaged across the width of the test patch as a function of test patch phase. It is clear that the averaged ODOG model output predicts a smooth transition in brightness and is in accord with the smooth transition in judged lightness reported by White and White (1985) as test patch phase is manipulated. Thus, the ODOG model is more successful in accounting for the data of White and White (1985) than is the T-junction rule.

Note again that the brightness across the test patches in these stimuli is not spatially homogenous, and neither is the ODOG model output. As before, the space-averaged model output is simply being used as a

convenient metric by which to predict the single-valued judgements of test patch lightness that were required of the subjects in the White and White (1985) study. In addition, although the White and White (1985) data represent judged lightness (whereas we are modeling brightness), it is expected that under the homogenous illumination conditions used in the White and White (1985) study, the measures of judged lightness and judged brightness would yield identical results (Arend & Spehar, 1993a,b).

7. Experiment 2: the point-by-point brightness profile of the White effect

The previous modeling demonstrations showed that the brightness profiles of the test patches in the White effect are not predicted to be homogeneous by the ODOG model. As discussed previously, Blakeslee and McCourt (1997) measured the brightness profiles of the test patches of GI and SBC stimuli using a point-by-point brightness matching technique. The spatial varia-

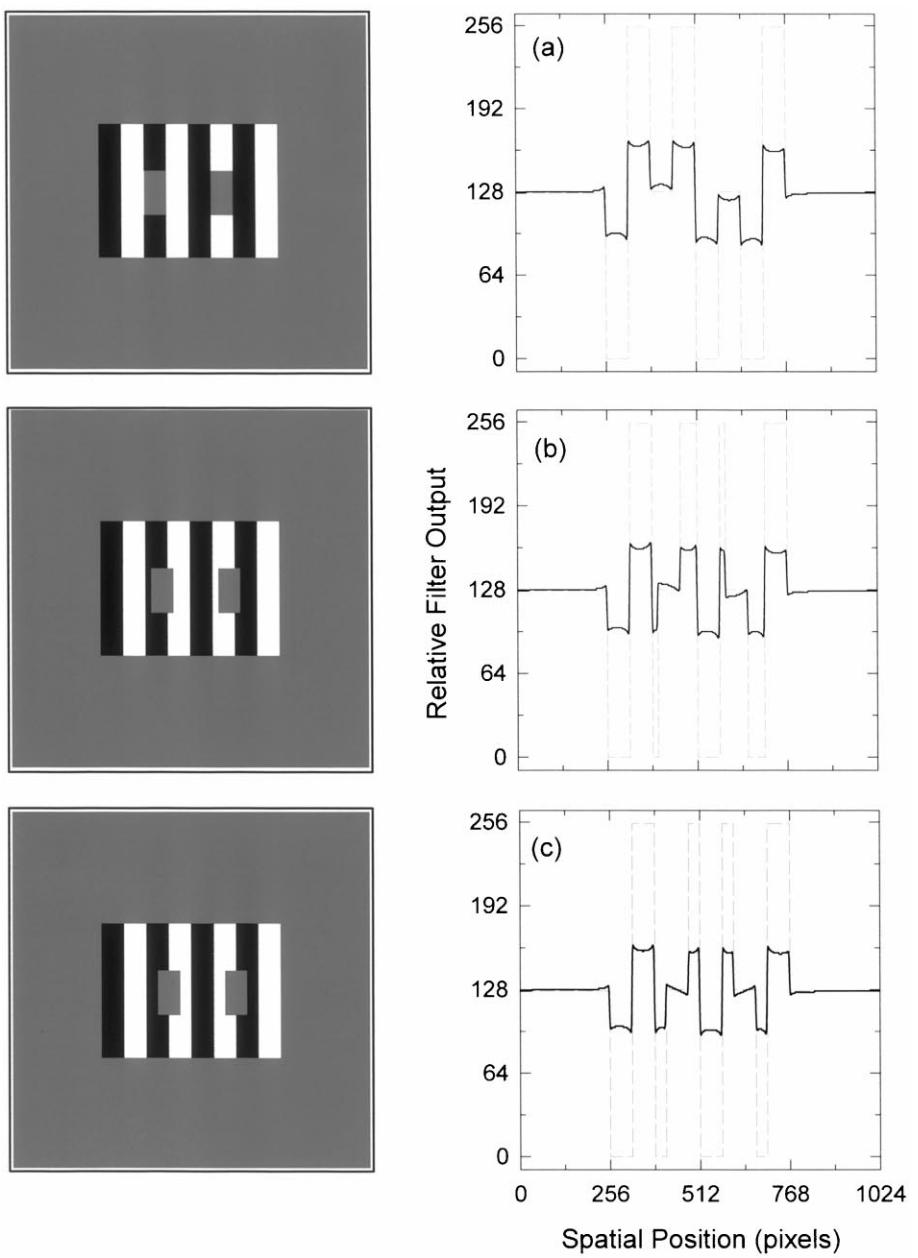

Fig. 6. The effect of test patch phase on the White effect using a 0.25 cyc/deg squarewave inducing grating with test patches measuring 2° in width and 4° in height. In the standard configuration (a) the gray test patch on the black bar is in the 0° phase relationship with the black bar and the gray test patch on the white bar is in the 180° phase relationship. In (b) the test patches have been shifted to the right by 45° phase angle. The test patches in (c) have been shifted by 90° phase angle. Right hand panels illustrate ODOG model output to the three displays, in which test patch spatial inhomogeneity is readily apparent.

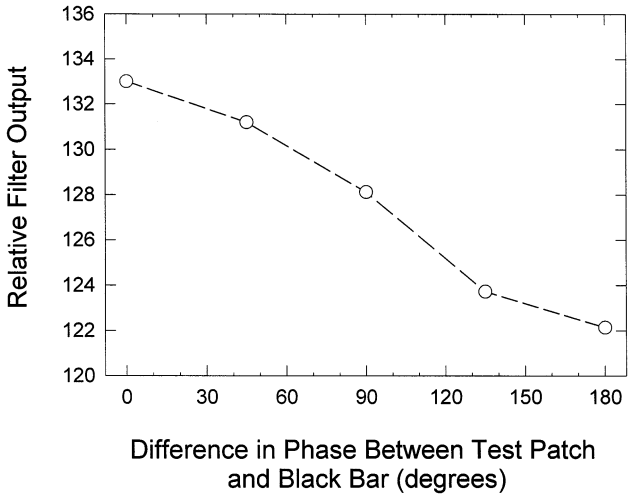

Fig. 7. The output of the ODOG model averaged across the width of the test patch plotted as a function of test patch phase. The averaged ODOG model output predicts a smooth transition in brightness.

tion of brightness was well predicted by the non-oriented DOG model. The ODOG model predictions for SBC and GI are similar to those of the DOG model and also account for the earlier point-by-point brightness matching data. In the following experiment point-by-point brightness matches were obtained for White stimuli identical to those used in the previous demonstration (Fig. 6). Brightness matches were measured at seven locations across each test patch and are compared with the ODOG model predictions for these stimuli.

7.1. Results and discussion

The symbols in the upper, middle and lower panels of Fig. 8 plot the mean point-by-point brightness matches (left ordinate) obtained for the stimulus configurations of the White effect appearing in the same page positions in Fig. 6. The upper panels correspond to the standard configuration of the White effect, while the middle and lower panels represent conditions in which the test patches have been displaced to the right by 16 and 32 pixels, respectively. Data from the two observers are plotted separately in the left and right columns and error bars represent the 95% confidence limits. The ODOG model output (right ordinate) to these stimuli is represented by the solid lines. It is clear that the model output closely corresponds to the observed spatial variation of brightness within the test patches of these stimuli, and that in no case can test patch brightness be described as spatially homogeneous.

8. Experiment 3: the Todorovic brightness effect

Todorovic (1997) and Zaidi et al. (1997) both showed that the relative brightness of test patches in the White effect can be predicted from the T-junction analysis. Todorovic (1997) introduced several novel stimuli that were also governed by this rule (Fig. 9b and c). Again, note that the gray test patches in Fig. 9b and c possess identical luminances and, like the test patches in the White effect, their brightness difference cannot be accounted for by isotropic contrast models that depend on the amount of black or white border either in contact with the test patch or in its general vicinity. Pessoa et al. (1998) parametrically varied the length of the arms of the test patches (crosses) in Todorovic stimuli like those shown in Fig. 9b–e and concluded that a T-junction analysis was not adequate to predict their results. They found that the brightness effect was greatly diminished when the arms of the cross exactly matched the perimeters of the squares (Fig. 9d) and then reversed direction when the arms extended beyond

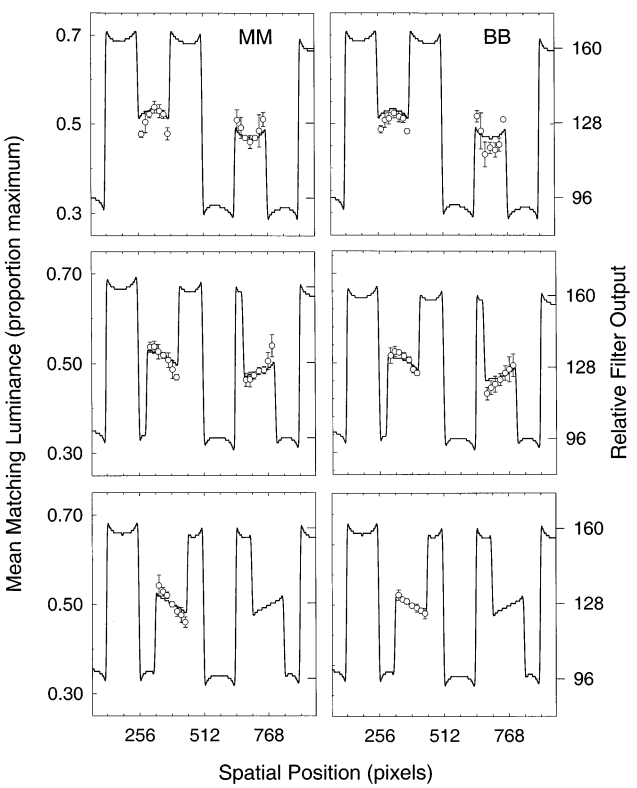

Fig. 8. Point-by-point brightness matches for phase-displaced test patches in the White effect. Symbols in the upper, central and lower panels plot point-by-point brightness matches (and 95% confidence intervals) obtained at seven locations across each test patch (as read against left ordinate). The stimuli from which these data were obtained are those shown in Fig. 6. Data from the two subjects are plotted separately in the left and right columns. Solid lines depict ODOG model output (read against right ordinate). ODOG model output closely parallels the observed brightness variations across the test patches in these stimuli.

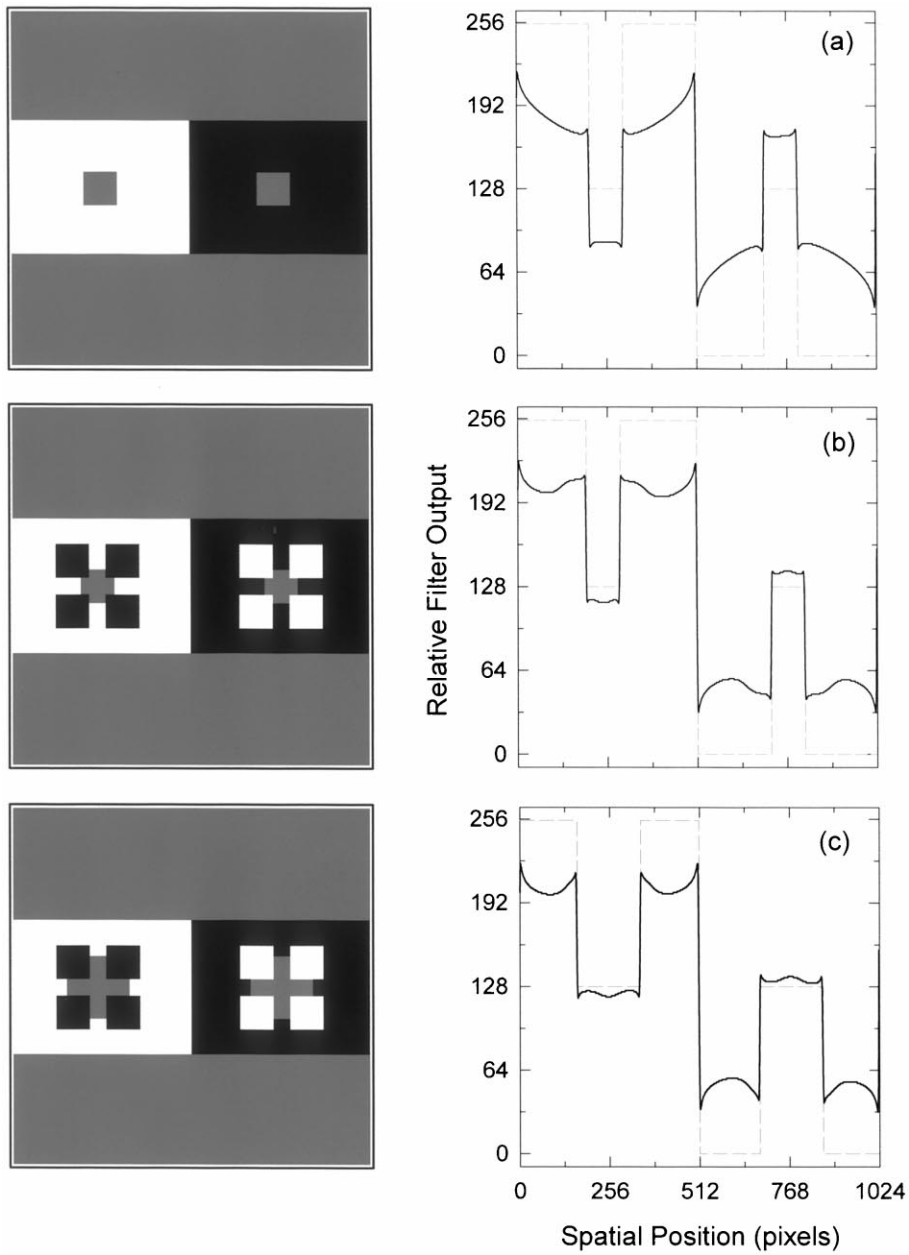

Fig. 9. The left-hand panels are a series of stimuli that include (a) a SBC stimulus with 3° test patches and (b–e) a set of stimuli similar to those employed by Pessoa et al. (1998). The first Todorovic stimulus in this series (b) is the same as the SBC stimulus (a), but with the superposition of the overlapping black and white 3° squares such that the test patch takes the form of a cross that is bordered by equal amounts of black and white. Notice that the test patch on the black background appears brighter than the test patch on the white background despite the fact that the test patch on the black background has the same amount of border contact with the black background and with the white overlapping squares. As the series unfolds (Fig. 9c–e) the only change is that the length of the arms of the crosses increases. The right-hand panels illustrate the ODOG model outputs for these stimuli.

the squares (Fig. 9e). As shown by Todorovic (1997), the T-junction analysis predicts the relative brightness of the test patches in displays where the arms of the crosses are short. In this configuration test patch brightness is most influenced by the backgrounds since the backgrounds are collinear with the test patches, i.e. together they form the stems of the T-junctions. The superimposed squares are largely ignored since they are the flanking regions, i.e. they form the tops of the T-junctions. Thus, the test patch on the black background appears brighter than the test patch on the white background. In the configuration in which the arms of the test patches exactly match the perimeters of the superimposed squares (Fig. 9d), the T-junction rule predicts the opposite relationship. The test patch on the black background is predicted to appear darker than the test patch on the white background since now the test region is collinear with the superimposed squares

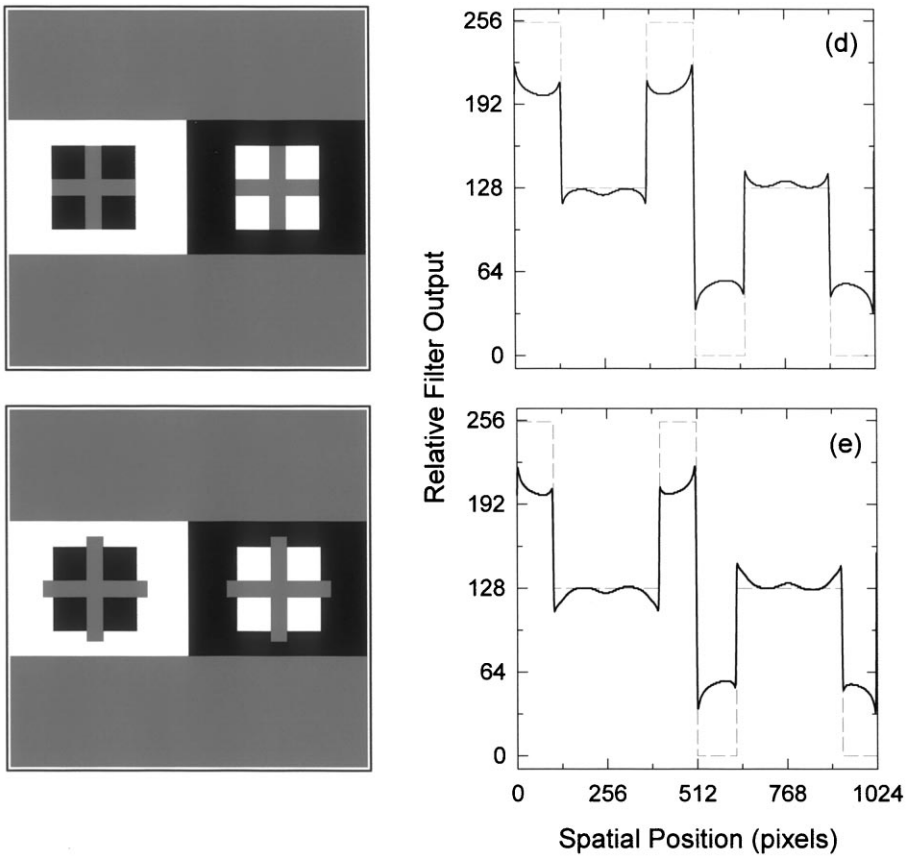

Fig. 9. (*Continued*)

(and is thus influenced by them) whereas the background is the flanking region. Finally, when the arms of the test patches extend beyond the superimposed squares, a T-junction analysis does not make a prediction for the test patch brightness since the test patches themselves are now the flanking regions.

Brightness matching was used to measure brightness induction in a series of stimuli that included a SBC stimulus with 3° test patches and a set of stimuli similar to those used by Pessoa et al. (1998). The first Todorovic stimulus in this series (Fig. 9b) is the same as the SBC stimulus (Fig. 9a), with superposed black and white 3° squares such that the test patch takes the form of a cross that is bordered by equal amounts of black and white. As the series progresses (Fig. 9c–e) the only change is that the length of the arms of the crosses increases.

8.1. Results and discussion

The stimuli and the ODOG model predictions for this experiment are shown in Fig. 9. As before, the model output contains spatial variation across the width of the test patches. Although such brightness variations were not measured psychophysically in this experiment, they were clearly observable to the subjects. The bars in Fig. 10 represent the brightness matching results (left ordinate); symbols plot the output of the model averaged across the extent of the test patch (right ordinate). Although the conditions labeled (SBC3) and (T1) also occur in Fig. 5 (labeled (SBC3) and (T)), the data in Fig. 10 represent independent replications of the previous measurements. The concordance with the previous results is excellent.

The ODOG model correctly predicts that the SBC stimulus produces the largest brightness effect (Figs. 9a and 10, (SBC3)). Note that there are no T-junctions in this stimulus and, therefore, there is no prediction from the T-junction analysis. The magnitude of induction is diminished (Figs. 9b and 10, (T1)) by the addition of the superimposed squares and this diminution is predicted by the ODOG model. The direction of the effect (i.e. that the test patch on the black background appears brighter) is predicted by both the T-junction rule and by the ODOG model. The brightness effect is further reduced when the arms of the test patches are lengthened (Figs. 9c and 10, (T2)), a result which is again captured by the ODOG model output. Note here that the T-junction structure of the stimulus has not changed from that of the previous condition; the amount of test patch border in contact with the superimposed squares as opposed to the background has

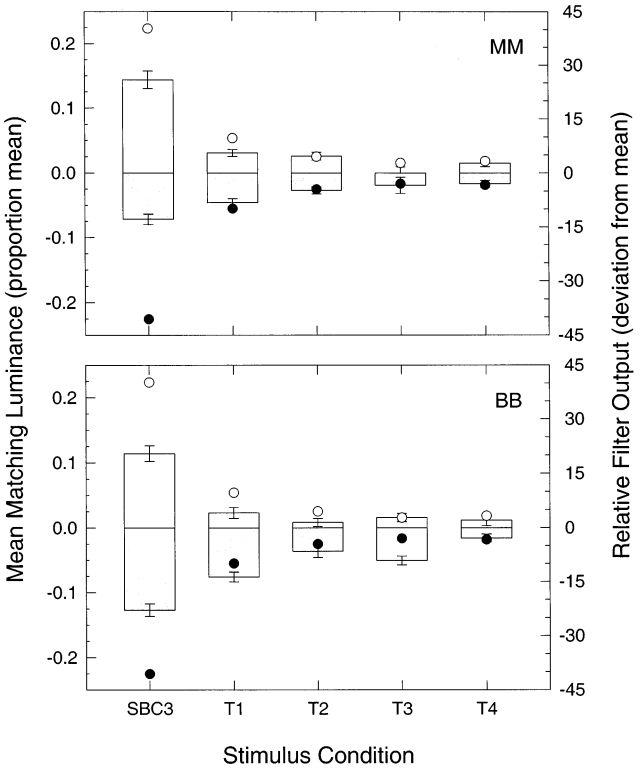

Fig. 10. The bar graph depicts brightness matching results (read against left ordinate) in the SBC and Todorovic displays. Symbols plot the output of the ODOG model averaged over the test patch (read against right ordinate). ODOG model output correctly predicts that the SBC stimulus produces the greatest brightness effect. The effect is diminished by the addition of superimposed squares in (T1), a result predicted by the ODOG model. Induction is further reduced in (T2), a stimulus in which the arms of the test patches are lengthened; this result is also captured by the ODOG model output. In condition (T3) the arms of the test patches exactly match the perimeters of the superimposed squares, and both subjects show a reversal of the direction of induction which *is* predicted by the T-junction rule, but not by the ODOG model. In (T4), when the arms of the crosses extend beyond the superimposed squares, both observers demonstrate a small effect in the original direction that is again in line with the predictions from the ODOG model.

increased, however, and the overall size of the cross has increased. In Figs. 9d and 10 (T3), the arms of the test patches exactly coincide with the perimeters of the superimposed squares. Interestingly, contrary to the report of Pessoa et al. (1998), we find that both subjects show a brightness reversal in this condition which *is* predicted by the T-junction rule. This reversal is not predicted by the ODOG model, however, whose output simply reflects a further decrease in the size of the effect, and fails to capture the reversal in direction. In the final condition where the arms of the crosses extend beyond the superimposed squares (Figs. 9e and 10, (T4)), both observers demonstrate a small effect in the original direction that is again in agreement with the output of the ODOG model. The T-junction rule does not make a prediction in this instance because the test patch is now the flanking region. Thus, the ODOG model generally accounts for the brightness of the test patches in this series of stimuli except in the condition in which the arms of the test patches exactly coincide with the perimeters of the superimposed squares. In this condition the ODOG model fails, and the T-junction analysis makes the correct prediction.

It may be instructive to inquire why the ODOG model fails in this instance despite the fact that its output generally captures the predictions of the T-junction analysis in the White effect and in the Todorovic demonstrations. Indeed, the ODOG model output succeeds where the T-junction analysis fails when accounting for the effects of manipulating test patch phase in the White effect, and in accounting for the observed brightness inhomogeneity within the test patches. Perhaps this is an instance where it *is* necessary to appeal to higher level perceptual processes, such as those related to perceptual grouping, in order to understand the results. Among the classic Gestalt grouping factors are proximity, good continuation, common fate and similarity (Gilchrist et al., 1999). Other grouping factors suggested to be important in determining brightness percepts include coplanarity (Gilchrist, 1980)—particularly when the luminance range within the stimulus is large—common illumination, T-junctions and X-junctions (Gilchrist et al., 1999). Note that in the series of stimuli depicted in Fig. 9, the shape of the test patch suggests different global interpretations of the stimulus. In Fig. 9b and c the test patch can be perceived as a cross, co-planar with and wedged between four abutting squares. A more compelling interpretation, however, is of a square situated in a recessed plane behind four superimposed squares. This percept may arise because T-junctions act as depth cues where the lateral region is seen as in front of the collinear regions (Todorovic, 1997). This interpretation also explains Fig. 9e where again the cross can be seen as sandwiched between the four squares, but where a more compelling interpretation is that of a cross occluding a complete underlying square. Fig. 9d is the only figure in which the cross is readily grouped with the squares as part of a single element; indeed it is difficult to interpret the squares and the cross as occupying different depth planes, or as not belonging together. Perhaps in this configuration a robust higher-level grouping cue causes perceived brightness to be more strongly influenced by the adjacent, co-planar squares than by the background. It is important to remember, however, that it has been convincingly demonstrated that the depth-inducing aspect of T-junctions is not responsible for the White or Todorovic effects, at least under conditions like those of the present experiment in which the luminance range is not too large (Zaidi et al.,1997; Todorovic, 1997). We suggest that while the low-level T-junction brightness rule described and discussed by

Zaidi et al. (1997) and Todorovic (1997) is captured to a first approximation by the elements of the ODOG model, there may be second-order grouping effects (to which T-junctions contribute) that can modify low-level brightness percepts under certain circumstances (Kingdom, Blakeslee & McCourt, 1997). This might explain why the ODOG model fails to account for the brightness matches in Fig. 9d, since the model does not incorporate such grouping factors.

The psychophysical results and ODOG modeling in the present paper strongly point to the conclusion that induced brightness phenomena such as SBC, GI, the White effect and the Todorovic demonstration primarily reflect operations performed by well-known early-stage cortical filters. The defining features of the ODOG model (e.g. multiscale spatial frequency sensitivity, orientation specificity and normalization) are response characteristics that are routinely observed at early cortical stages of visual processing in both cat and monkey (Geisler & Albrecht, 1995; Gilbert et al., 1996; Rossi et al., 1996;). It should be noted, however, that the incorporation of additional response non-linearities into the ODOG model is expected to be required to accommodate more brightness data.

Although the brightness percepts resulting from low-level filtering operations may, under certain circumstances, be modified by higher-order visual processes (see Fig. 9d), the present results argue persuasively against the necessity of invoking such higher-order processes to explain the origin and relative magnitude of the basic brightness effects measured under the conditions of the present study. While subtle influences on brightness due to the outcomes of higher-level inferential processes, such as transparency (Adelson, 1993; Kingdom, Blakeslee & McCourt, 1997), perceived stereo depth (Schirillo & Shevell, 1993; Spehar, Gilchrist & Arend, 1995), perceived pictorial depth or shape (Knill & Kersten, 1991; Adelson, 1993; Buckley, Frisby & Freeman, 1994; Wishart, Frisby & Buckley, 1997) perceived 'belongingness' (Agostini & Proffitt, 1993) and co-planarity (Gilchrist, 1980; Gilchrist et al., 1999) have been demonstrated, further research is required to clearly determine the circumstances under which these factors exert an influence on brightness and to determine the magnitudes of these effects.

References

Adelson, E. H. (1993). Perceptual organization and the judgement of brightness. *Science*, *262*, 2042–2044.

Agostini, T., & Proffitt, D. R. (1993). Perceptual organization evokes simultaneous lightness contrast. *Perception*, *22*, 263–272.

Arend, L. E., & Spehar, B. (1993a). Lightness, brightness, and brightness contrast: 1. Illuminance variation. *Perception and Psychophysics*, *54*(4), 446–456.

Arend, L. E., & Spehar, B. (1993b). Lightness, brightness, and brightness contrast: 2. Reflectance variation. *Perception and Psychophysics*, *54*(4), 457–468.

Blakeslee, B., & McCourt, M. E. (1997). Similar mechanisms underlie simultaneous brightness contrast and grating induction. *Vision Research*, *37*, 2849–2869.

Buckley, D., Frisby, J. P., & Freeman, J. (1994). Lightness perception can be affected by surface curvature from stereopsis. *Perception*, *23*, 869–881.

Cornsweet, T. N., & Teller, D. (1965). Relation of increment thresholds to brightness and luminance. *Journal of the Optical Society of America*, *55*(10), 1303–1308.

DeValois, R. L., & DeValois, K. K. (1988). *Spatial Vision*. New York: Oxford University Press.

DeValois, R. L., & Pease, P. L. (1971). Contours and contrast: responses of monkey lateral geniculate cells to luminance and color figures. *Science*, *171*, 694–696.

Foley, J. M., & McCourt, M. E. (1985). Visual grating induction. *Journal of the Optical Society of America A*, *2*, 1220–1230.

Geisler, W. S., & Albrecht, D. G. (1995). Bayesian analysis of identification performance in monkey visual cortex: nonlinear mechanisms and stimulus certainty. *Vision Research*, *35*, 2723–2730.

Georgeson, M. A., & Sullivan, G. D. (1975). Contrast constancy: deblurring in human vision by spatial frequency channels. *Journal of Physiology* (*London*), *252*, 627–656.

Gilbert, C. D., Das, A., Ito, M., Kapadia, M., & Westheimer, G. (1996). Spatial integration and cortical dynamics. *Proceedings of the National Academy of Sciences USA*, *93*, 615–622.

Gilchrist, A. (1980). When does perceived lightness depend on perceived spatial arrangement. *Perception and Psychophysics*, *28*, 527–538.

Gilchrist, A., Bonato, F., Annan, V., & Economou, E. (1998). Depth, lightness (and memory). *Investigative Ophthalmology and Visual Science* (*Supplement*), *39*, S671.

Gilchrist, A., Kossifydis, C., Bonato, F., Agostini, T., Cataliotti, J., Li, X., Spehar, B., Annan, V., & Economou, E. (1999). An anchoring theory of lightness perception. *Psychological Review* (in press).

Grossberg, S., & Todorovic, D. (1988). Neural dynamics of 1-D and 2-D brightness perception: A unified model of classical and recent phenomena. *Perception and Psychophysics*, *43*, 241–277.

Heinemann, E. G. (1955). Simultaneous brightness induction as a function of inducing and test-field luminances. *Journal of Experimental Psychology*, *50*, 8996.

Heinemann, E. G. (1972). Simultaneous brightness induction. In D. Jameson, & L. M. Hurvich, *Handbook of Sensory Physiology*, *VII-4 Visual Psychophysics*. Berlin: Springer-Verlag.

Kingdom, F. A. A. (1997). Simultaneous contrast: the legacies of Hering and Helmholtz. *Perception*, *26*, 673–677.

Kingdom, F. A. A., Blakeslee, B., & McCourt, M. E. (1997). Brightness with and without perceived transparency: when does it make a difference? *Perception*, *26*, 493–506.

Kingdom, F. A. A., & Moulden, B. (1988). Border effects on brightness: a review of findings, models and issues. *Spatial Vision*, *3*(4), 225–262.

Kingdom, F. A. A., & Moulden, B. (1992). A multi-channel approach to brightness coding. *Vision Research*, *32*, 1565–1582.

Knill, D. C., & Kersten, D. (1991). Apparent surface curvature affects lightness perception. *Nature*, *351*, 228–230.

McCourt, M. E. (1982). A spatial frequency dependent grating-induction effect. *Vision Research*, *22*, 119–134.

McCourt, M. E. (1994). Grating induction: a new explanation for stationary visual phantoms. *Vision Research*, *34*, 1609–1618.

McCourt, M. E., & Blakeslee, B. (1994). A contrast matching analysis of grating induction and suprathreshold contrast perception. *Journal of the Optical Society of American A*, *11*, 14–24.

Moulden, B., & Kingdom, F. A. A. (1989). White's effect: a dual mechanism. *Vision Research*, *29*, 1245–1259.

Moulden, B., & Kingdom, F. A. A. (1991). The local border mechanism in grating induction. *Vision Research*, *31*, 1999–2008.

Paradiso, M. A., & Hahn, S. (1996). Filling-in percepts produced by luminance modulation. *Vision Research*, *36*, 2657–2663.

Paradiso, M. A., & Nakayama, K. (1991). Brightness perception and filling-in. *Vision Research*, *31*, 1221–1236.

Pessoa, L., Baratoff, G., Neumann, H., & Todorovic, D. (1998). Lightness and junctions: variations on White's display. *Investigative Ophthalmology and Visual Science* (*Supplement*), *39*, S159.

Pessoa, L., & Ross, W. D. (1996). A contrast/filling in model of 3-D lightness perception: Benary cross, White's effect and coplanarity. *Investigative Ophthalmology and Visual Society of America A*, *10*, 2442–2452.

Rossi, A. F., & Paradiso, M. A. (1996). Temporal limits of brightness induction and mechanisms of brightness perception. *Vision Research*, *36*, 1391–1398.

Rossi, A. F., Rittenhouse, C. D., & Paradiso, M. A. (1996). The representation of brightness in primary visual cortex. *Science*, *273*, 1104–1107.

Schirillo, J., & Shevell, S. K. (1993). Lightness and brightness judgements of coplanar retinally noncontiguous surfaces. *Journal of the Optical Society of America A*, *10*, 2442–2452.

Shapley, R., & Enroth-Cugell, C. (1984). Visual adaptation and retinal gain-controls. *Progress in Retinal Research*, *3*, 263–346.

Shapley, R., & Reid, R. C. (1985). Contrast and assimilation in the perception of brightness. *Proceedings of the National Academy of Science USA*, *82*, 5983–5986.

Spehar, B., Gilchrist, A. L., & Arend, L. E. (1995). The critical role of relative luminance relations in White's effect and grating induction. *Vision Research*, *35*, 2603–2614.

Taya, R., Ehrenstein, C., & Cavonius, R. (1995). Varying the strength of the Munker–White effect by stereoscopic viewing. *Perception*, *24*, 685–693.

Todorovic, D. (1997). Lightness and junctions. *Perception*, *26*, 379–395.

Watt, R. J., & Morgan, M. J. (1985). A theory of the primitive spatial code in human vision. *Vision Research*, *25*, 1661–1674.

White, M. (1979). A new effect of pattern on perceived lightness. *Perception*, *8*, 413–416.

White, M. (1981). The effect of the nature of the surround on the perceived lightness of grey bars within square-wave test gratings. *Perception*, *10*, 215–230.

White, M., & White, T. (1985). Counterphase lightness induction. *Vision Research*, *25*, 1331–1335.

Wilson, H. R., & Bergen, J. R. (1979). A four mechanism model for threshold spatial vision. *Vision Research*, *19*, 19–32.

Wishart, K. A., Frisby, J. P., & Buckley, D. (1997). The role of 3-D surface slope in a lightness/brightness effect. *Vision Research*, *37*, 467–473.

Yund, E. W., & Armington, J. C. (1975). Color and brightness contrast effects as a function of spatial variables. *Vision Research*, *15*, 917–929.

Yund, E. W., Snodderly, D. M., Hepler, N. K., & DeValois, R. L. (1977). Brightness contrast effects in monkey lateral geniculate nucleus. *Sensory Processes*, *1*, 260–271.

Zaidi, Q. (1989). Local and distal factors in visual grating induction. *Vision Research*, *29*, 691–697.

Zaidi, Q., Spehar, B., & Shy, M. (1997). Induced effects of background and foregrounds in three-dimensional configurations: the role of T-junctions. *Perception*, *26*, 395–408.